

Simulations of Buoyant Bubbles in Galaxy Clusters

M.Brüggen^{1,2}

m.brueggen@iu-bremen.de

ABSTRACT

It is generally argued that most clusters of galaxies host cooling flows in which radiative cooling in the centre causes a slow inflow. However, recent observations by Chandra and XMM conflict with the predicted cooling flow rates. Here we report highly resolved hydrodynamic simulations which show that buoyant bubbles can offset the cooling in the inner regions of clusters and can significantly delay the deposition of cold gas. The subsonic rise of bubbles uplifts colder material from the central regions of the cluster. This colder material appears as bright rims around the bubbles. The bubbles themselves appear as depressions in the X-ray surface brightness as observed in a growing number of clusters.

Subject headings: galaxies: active - galaxies: clusters: cooling flows - X-rays: galaxies

1. Introduction

The X-ray surface brightness of many clusters of galaxies shows a strong central peak which is generally interpreted as the signature of a cooling flow (Cowie & Binney 1977, Fabian & Nulsen 1977, Sarazin 1988, Fabian 1994). However, the simple cooling flow model conflicts with a growing number of observations that show that while the temperature is declining in the central region, gas with a temperature below ~ 1 keV is significantly less abundant than predicted (Peterson et al. 2001, Tamura et al. 2001). It has been shown that star formation rates as inferred from observations only amount to a few percent of the predicted mass deposition rates of $1 - 1000 M_{\odot}/\text{yr}$ (e.g. McNamara 1997, Crawford et al. 1999). Moreover, spectral evidence gathered by XMM-Newton has shown inconsistencies of the observed spectra with those predicted by cooling flow models (Böhringer et al. 2002).

¹International University Bremen, Campus Ring 1, 28759 Bremen, Germany

²Max-Planck Institut für Astrophysik, Karl-Schwarzschild-Str 1, 85740 Garching, Germany

Recently, two main candidates for the heating of the gas in the central regions of clusters have emerged: (i) heating by outflows from active galactic nuclei (AGN) (Tabor & Binney 1993, Churazov et al. 2001, Brüggen et al. 2002, Brüggen & Kaiser 2002, Basson & Alexander 2002, Reynolds, Heinz, & Begelman 2001), and (ii) transport of heat from the outer regions of the cluster by thermal conduction (Zakamska & Narayan 2002, Narayan & Medvedev 2001, Fabian, Voigt & Morris 2002, Ruszkowski & Begelman 2002, Voigt et al. 2002, Gruzinov 2002, Bertschinger & Meiksin 1986). A third possibility that has been discussed is heating by magnetic fields through reconnection (e.g. Soker & Sarazin 1990).

In this paper we will consider the first scenario. Radio-loud active galactic nuclei (AGN) drive strong outflows in the form of jets that inflate bubbles or lobes. The lobes are filled with hot plasma, and can heat the cluster gas in various ways. In the case of very energetic jets, the expansion of the lobes will be supersonic, and the resulting strong shock will heat and compress the gas. However, there is mounting evidence that weaker jets, which are presumably much more common, do not lead to efficient shock heating. Nevertheless, they still produce pockets of low-density gas that displace the hot intra-cluster medium (ICM) and thus appear as depressions in the X-ray surface brightness. High-resolution X-ray observations of cooling flow clusters with Chandra have revealed a multitude of X-ray holes on scales < 50 kpc, often coincident with patches of radio emission, e.g. in Abell 2052 (Blanton et al. 2001), Perseus (Böhringer et al. 1993, Churazov et al. 2000, Fabian et al. 2000), Cygnus A (Wilson, Young, & Shopbell 2000 and Carilli, Perley, & Harris 1994), Abell 2597 (McNamara et al. 2001), MKW3s (Mazzotta et al. 2002), RBS797 (Schindler et al. 2001), HCG62 (Vrtilek et al. 2000) and Centaurus A (Saxton, Sutherland, & Bicknell 2001). In addition to radio-bright cavities, radio-faint “ghost” cavities have been found, e.g. in Perseus, which presumably date from previous radio episodes of the AGN. The pressure support in the cavities is not well understood. In Abell 2052 the external gas pressure is about 10 times higher than the internal equipartition pressure. The cavities found in MKW3s, however, are filled with hot thermal gas that provides pressure support against the ICM and the radio observations of Hydra A also suggest that the bubbles are in local pressure equilibrium with the surroundings. The ubiquity of cavities in clusters means that they must be relatively long-lived and that the majority must be in rough pressure balance with their surroundings. However, the source of this pressure, the structure of the magnetic fields inside the bubbles and the equation of state of the hot plasma are still uncertain.

Chandra images of Hydra A, Perseus and Abell 2052 show soft X-ray emission from the rims of the bubbles which imply that the gas around the rims of these bubbles is colder and not hotter than the ambient gas (e.g. Fabian et al. 2000, 2001, Nulsen et al. 2002).

The existence of these cold rims is taken as evidence that the gas has not been shocked during the inflation of the bubbles but that the cold rims consist of low-entropy gas that has been displaced from the centre of the cluster (Brighenti & Mathews 2002). Therefore, the radio lobes must have expanded gently into the ICM. The buoyant rise and the subsequent mixing of high-entropy gas with the cluster material can lead to a significant re-structuring of the inner regions of a cooling flow (e.g., Brüggen & Kaiser 2002, Basson & Alexander 2002).

Assuming that a typical central galaxy produces 10-100 bubbles in its life time, each carrying an energy of up to 10^{59} ergs, the total energy in bubbles can be comparable to the thermal energy of the X-ray emitting plasma in the inner cluster regions (McNamara 2002). Moreover, there is evidence that the total power in radio jets is substantially larger than the radio power of the lobes that they feed (Bicknell & Begelman 1996). Thus the question arises of where the energy ultimately goes and what fraction of the energy is deposited into the ICM. This is the question that is addressed in this paper.

Both, the rise and the mixing are complex processes that are difficult to treat on the basis of analytical estimates alone. We therefore performed highly resolved two-dimensional hydrodynamic simulations of buoyant gas in a typical cluster environment similar to previous simulations of lower resolution. Only two-dimensional simulations were performed because our primary aim was to achieve a very high spatial resolution in order to minimize the effects of numerical diffusivity that have hampered previous simulations. This was also aided by the use of an adaptive grid that places resolution elements only where they are needed, such that an effective resolution of 2048 times 2048 elements could be achieved. Experience has shown that large-scale transport properties are not very different in two dimensional and three-dimensional simulations, so we expect our conclusions to hold even for the three-dimensional reality.

In this paper, we will extend the work presented in Brüggen & Kaiser 2002. Apart from a much more detailed analysis, we have extended previous work by simulating an ambipolar jet in the entire cluster compared to merely a section of the cluster. Thus, any artificial surfaces of symmetry are avoided (as also in Reynolds, Heinz, & Begelman 2001; Basson & Alexander 2002) and the amount of global, distributed heating can be studied. Moreover, we ran the simulations for a long physical time, namely for much longer than the central cooling time of the cluster. We also included radiative cooling and treated the radio plasma and the ambient plasma as separate fluids with different equations of state.

2. Model

The initial density was assumed to follow the dark matter, which is given by a modified NFW profile (Navarro et al. 1997)

$$\rho(r) = \frac{\rho(0)r_s}{(r + r_s)(1 + r/r_c)^2}, \quad (1)$$

where r is the distance from the centre, r_c the core radius and r_s a softening radius, which we assumed to be proportional to the core radius, i.e. we chose $r_s = r_c/30$. The parameters of our model are $n_e(0) = 0.3 \text{ cm}^{-3}$, $r_c = 300 \text{ kpc}$, $r_s = r_c/30$ and the baryon fraction is 10%. The temperature and pressure are calculated assuming initial hydrostatic equilibrium. The initial model of our simulations is shown in Fig. 1. Thus our model has got a central cooling time of around 20 Myrs.

Inspired by a growing number of observations of X-ray cavities in the ICM, we introduce heating at off-centre sites by ad-hoc bubbles. To mimic the energy input by a jet, hot, buoyant gas was injected continuously into two small spherical regions which lie on opposite sides of the centre of the cluster. The injection region had a radius of 0.5 kpc, and the rate of energy input was $L = 6 \times 10^{44}$ which is a typical kinetic luminosity of a radio jet (Owen, Eilek, & Kassim 2000). This rate is also near the maximum rate that allows the bubbles to detach themselves from the injection region in the course of their rise. For higher luminosities a large bubble is inflated that evacuates most of the cluster centre before it can rise and become detached from the injection region. Which mechanism is responsible for tuning the energy of the radio jets remains unclear. The energy input was switched off after 208 Myr which is estimated to be a typical time for a recurring FRI source (Saxton, Sutherland, & Bicknell 2001). We assumed that the temperature of the injected fluid was 100 times greater than the temperature of the ambient fluid at the same location and that the gas had zero initial velocity.

We treated the hot gas in the bubbles and the ambient cluster gas as two separate fluids which obey two separate equations of state. The ICM was assumed to obey a $\gamma = 5/3$ polytropic equation of state. However, the equation of state within the bubbles is unknown. We assume that the magnetic field within the rarefied bubbles is tangled on small scales and can be approximated together with the relativistic particles by a $\gamma = 4/3$ equation of state. The ambient gas and the gas in the bubbles is allowed to cool via thermal bremsstrahlung and line radiation. The cooling function of the gas was taken from Sarazin (1986) and Raymond (1976) (see Fig. 2). We have neglected the synchrotron losses of the radio plasma assuming

it to be very hot so that it hardly cools at all. Finally, magnetic fields have been ignored.

The simulations were performed with the FLASH code using an explicit solver based on the piecewise-parabolic method (PPM). This method is accurate to second order in both time and space and uses a monotonicity constraint and contact steepening. For a detailed description of the FLASH code, the reader is referred to Fryxell et al. (2000). Radiative cooling was treated explicitly with a separate timestep limiter. The code uses an adaptive grid which refines and derefines the computational mesh as needed. The computational domain span $140 \text{ kpc} \times 140 \text{ kpc}$ and was centred on the centre of the cluster. The effective resolution in our simulations was 2048×2048 zones. On all boundaries outflow conditions were enforced. All simulations were run on 16 processors on an SGI Origin 3000 and on an IBM Regatta system.

3. Results and Discussion

Figure 3 shows logarithmic contour plots of the density at 84, 167, 252 and 336 Myr after the start of the energy injection. In the last two picture the injection of energy has ceased. One can see how the buoyant plume rises upwards while Rayleigh-Taylor instabilities form mushroom-shaped plumes on the bubble surfaces. Kelvin-Helmholtz instabilities at the boundary between the radio plasma and the ICM leads to the formation of tori and the shedding of vortex rings. The tori form when the rarefied gas in the wake of the bubble penetrates the bubble from below and makes contact with the thermal gas on the upper side of the bubble (Saxton, Sutherland, & Bicknell 2001). The rising tori cause the thermal gas to circulate around them. The velocity of the bubbles increase with increasing distance from the centre as expected (Churazov et al. 2001). A stream of denser gas trails the bubbles and marks their path. The largest bubbles are found at the leading edge of the buoyant gas. One can see that as the bubble rises upwards the space between the top bubble and the centre gets scattered with smaller radio bubbles and vortex rings. Thus the bubbles are shredded producing a broad distribution of sizes and velocities where the smaller bubbles rise more slowly. The final fate of the bubbles is, i.e. whether they will rise out of the cluster before they are mixed microscopically into the ICM, is difficult to tell from these simulations and will depend crucially on the strength and structure of the magnetic fields inside the bubbles. Therewhilst denser gas is pushed outwards despite the effect of radiative cooling which would cause the gas to flow inwards. It is remarkable that bubbles are found at fairly large distances from the jet axis leading to a broad distribution of bubbles. From an injection region of width of 1 kpc the bubbles spread laterally to distances of up to 30

kpc - which corresponds to 1/10th of the core radius - from the axis.

Thus the positions of X-ray cavities do not always allow simple inferences on the orientation of the jet axis. In some cases bubbles have been observed that are located off-centre from the current jet axis and this has led to suggestions that the jet axis has turned. However, this does not always have to be the case. Some bubbles may merely have migrated away from the axis due to instabilities. This may explain why in some clusters, such as Perseus, the X-ray holes appear to be randomly distributed about the centre.

In Fig. 4 we show a map of the X-ray surface brightness at a time of 100 Myrs after the start of the simulation. For this purpose we have rotated the 2D output around the jet axis and integrated the bremsstrahlung emissivity along lines of sight. Since the bremsstrahlung emissivity goes as $n_e^2 T^{1/2}$ the X-ray maps show a very luminous core. Therefore, the cavities are more difficult to observe at the centre but become more prominent once they have reached a height of roughly a tenth of the core radius. The surface brightness image also shows a bias towards the larger bubbles while many of the smaller structures remain obscured.

Figure 5 shows a contour plot of the temperature at 120 Myr after the start of the energy injection. A trunk of colder gas is uplifted in the wake of the bubbles. One can note how colder gas has been entrained and is lifted upwards by the bubbles. As mentioned in Sec. I, observations have shown that gas immediately around the bubbles is colder than the ambient gas (e.g. Fabian et al. 2000, 2001, Nulsen et al. 2002). In Fig. 6 we show an enlarged contour plot of the temperature in the vicinity of the bubbles. One can clearly see how entrained, colder gas from the central regions is being pushed out by the buoyant bubbles. The bubbles are surrounded by colder, low-entropy gas which appears bright in X-ray images. These rims have got widths of $\sim 1 - 5$ kpc. Their widths decrease with increasing distance from the centre which can be attributed to three factors: First, as the bubbles accelerate, they compress the gas in front of them; second, the material in the rims cools faster than the ambient ICM and third, some of the rim material is being mixed into the ambient ICM. The rims are 20% to 40% cooler than the adjacent thermal gas which is consistent with observations (Nulsen et al. 2002). They also become cooler with their distance from the centre because they cool faster. Our simulations confirm the suggestion by Brighenti & Mathews (2002) who identified the source of the bright rims in low-entropy gas from the cluster centre.

We have found that without cooling the average temperature in the core goes up because hotter material from outer regions is mixed into the core and the expanding bubbles are performing work on the ambient medium (Brüggen & Kaiser 2002). For the simulations

presented here we have plotted the temperature evolution of the cluster gas in Fig. 7. The temperature has been averaged over spherical shells of thickness 10 kpc about the cluster centre. Material with a specific entropy below a suitably chosen threshold can be identified as ambient fluid, as opposed to bubble fluid which has got a higher entropy. This enables us to study the temperature evolution of the original cluster gas alone (Reynolds, Heinz, & Begelman 2001). Only the ambient cluster gas has been included in the average shown in Fig. 7. In the right panel of Fig. 7 we have plotted the temperature evolution of the same cluster without heating by bubbles. The comparison shows clearly how, over the timescales considered here, the bubbles manage to keep the temperature in the central regions of the cluster constant (or even raise them). Fig. 8 shows the evolution of the specific entropy in the cluster. Again, the entropy has been averaged over spherical shells of thickness 5 kpc. One can notice how in all but the innermost shells the entropy is kept at a fairly constant level or even rises despite the cooling. This effect of the rising bubbles persists for a time of more than 400 Myrs which is twice as long as the time for which the jet was active and approximately the sound crossing time of the core radius r_c . In the cooling-flow model, mass deposition is greatest in the core, where the cooling time drops sharply. The mass that condenses out in the cores ceases to provide pressure support, and thus causes a slow inflow. Therefore, the cooling flow can be delayed significantly if the cooling of gas in the central regions can be halted.

As pointed out by Churazov et al. (2002) the work done by the rising bubble can be estimated by considering the enthalpy of the bubble during adiabatic expansion

$$H = \frac{\gamma}{\gamma - 1} pV = H_0 \left(\frac{p}{p_0} \right) , \quad (2)$$

where H_0 and p_0 are the enthalpy and pressure at the initial position. Taking a typical pressure profile, approximately half the energy is lost at a distance of ~ 20 kpc from the origin. This work goes mainly into $p dV$ work on the ambient medium, kinetic and potential energy of the entrained gas and sound waves. Given the steep entropy profile in the inner regions of the cluster, large masses of entrained gas cannot travel a long distance with the rising bubbles, and therefore most of the energy will stay in the cluster.

Sound waves will only have a minor share in the energy lost since the ratio between the energy in sound waves over the dissipated energy for subsonic turbulence goes as

$$\frac{\epsilon_s}{\epsilon_d} = \left(\frac{v}{c_s} \right)^5 \ll 1 . \quad (3)$$

Clearly, the lifetime of the activity of the central AGN is short compared to the evolutionary timescale of the cluster gas. Therefore, once the AGN stops supplying energy to the buoyant bubbles, the cluster gas will settle down once again and a full cooling flow may be re-established. The cooling gas flowing to the centre of the cluster may then trigger a further active phase of the AGN. Thus a self-regulating process with cooling periods alternating with brief bursts of AGN activity may be established. The rising bubbles uplift colder material from near the AGN and thus disrupt the supply of fresh fuel for the radio jets. This feedback mechanism might automatically regulate the power of the radio jets. The details of this mechanism remain unclear but it is potentially important as it might provide an upper mass limit for galaxies. For more on feedback between gas accretion and radio power see, e.g. Quilis, Bower, & Balogh (2001), Voit & Bryan (2001), Ruszkowski & Begelman (2002).

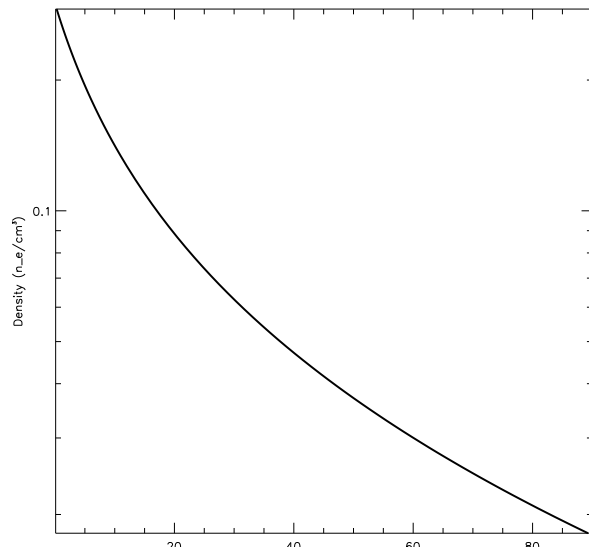
It has been found that 71 % of all cD galaxies at the centres of cooling-flow clusters show evidence of radio activity (Burns 1990). This fraction is higher than in non-cooling flow galaxies which again points towards the existence of some form of feedback mechanism. If all AGN at the centres of cooling flows go through activity cycles of constant length, t_{on} , separated by periods of quiescence, again of constant length, t_{off} , then these observations imply that $t_{\text{off}} < 0.41 t_{\text{on}}$. Figure 8 indicates that the simulated cluster starts to relax back to its original state after a time of ~ 400 Myr and returns to a cooling dominated inflow. Thus it gets close to a configuration similar to that at which the AGN activity started. Despite having chosen one particular realisation of the gas distribution inside the cluster, these findings are insensitive to the details of the cluster model. Experiments with other cluster models have yielded very similar results.

Cosmological simulations as well as observations suggest that the gas in many clusters may not be in an equilibrium state, in contrast to what we assumed in our simulation. However, gas flows of low Mach numbers within a cluster are unable to impede the rise of the bubbles, and are more likely to increase than to decrease the mixing. Moreover, clusters that are far from hydrostatic equilibrium are generally not expected to host cooling flows.

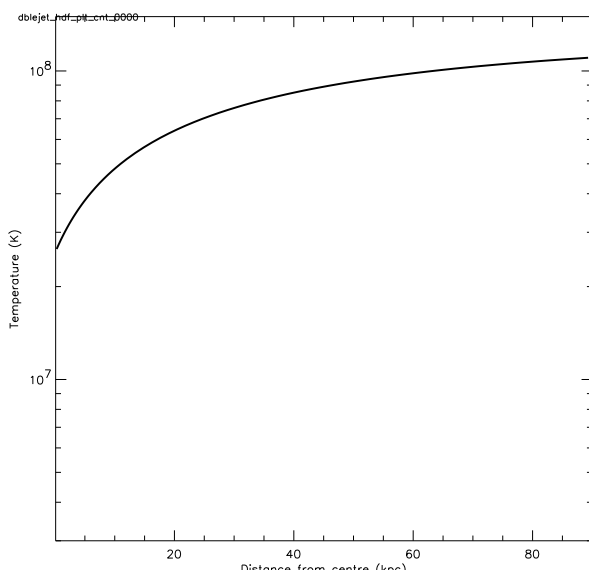
In summary, we have found that bubbles can heat the cluster core by input of mechanical energy. The effect of the bubbles on the ICM consists of heating via PdV work and redistribution of mass via buoyancy-driven mixing. For realistic parameters the heating is shown to be sufficient to balance radiative cooling and to disrupt, at least temporarily, the cooling flow. Thus a significant fraction of the energy residing in radio lobes can be dissipated in the cooling flow. Clearly, heating by AGN will not account for the entirety of

the missing gas in cooling flows but it is shown to be an efficient and common mechanism which introduces heat into the ICM. During their rise in the cluster potential, the bubbles expand and produce depressions in the X-ray surface brightness. Moreover, hydrodynamical instabilities produce a broad distribution of smaller bubbles and vortices. Bright rims are a common feature around buoyant bubbles and consist of colder gas that has been uplifted from the centre. The bright rims seen in our simulations are consistent with those found in observations.

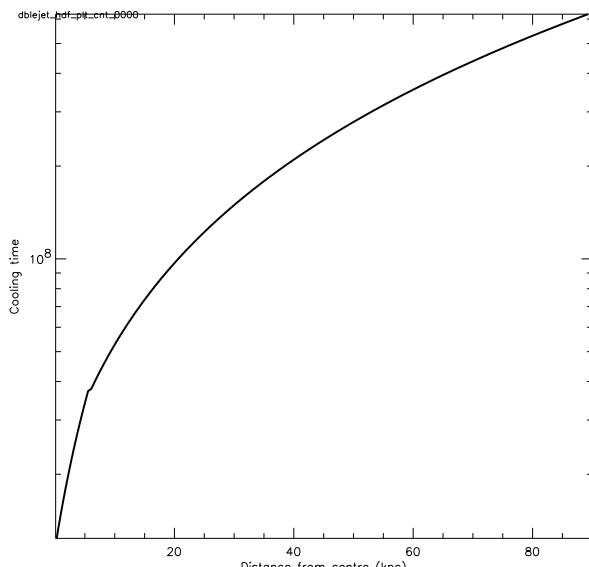
The software used in this work was in part developed by the DOE supported ASCI/Alliances Center for Thermonuclear Flashes at the University of Chicago. I thank Christian Kaiser, Bill Forman and Eugene Churazov for helpful discussions.



time = 0.000 Gyr
number of blocks = 18, AMR levels = 5



time = 0.000 Gyr
number of blocks = 18, AMR levels = 5



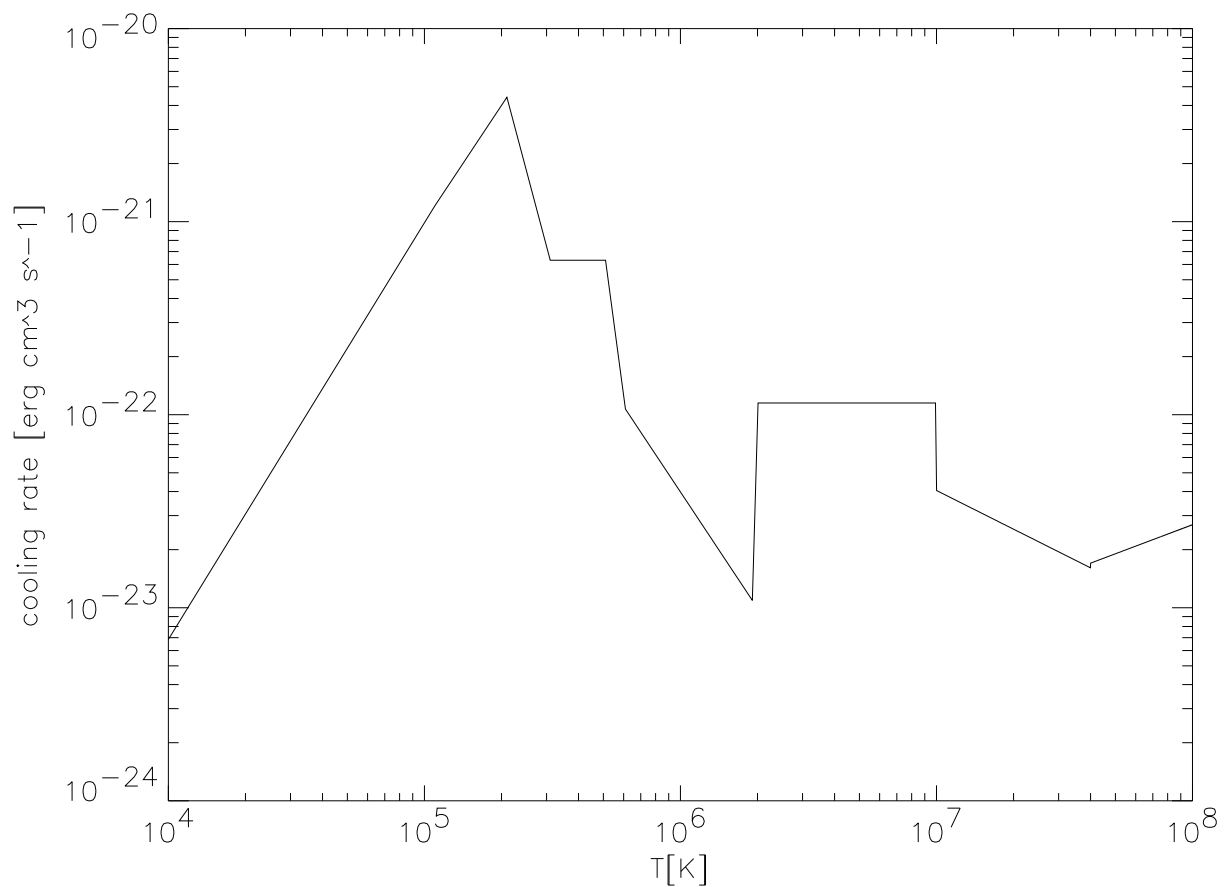


Fig. 2.— Approximate cooling rate versus temperature as given by Sarazin (1986) and Raymond (1976).

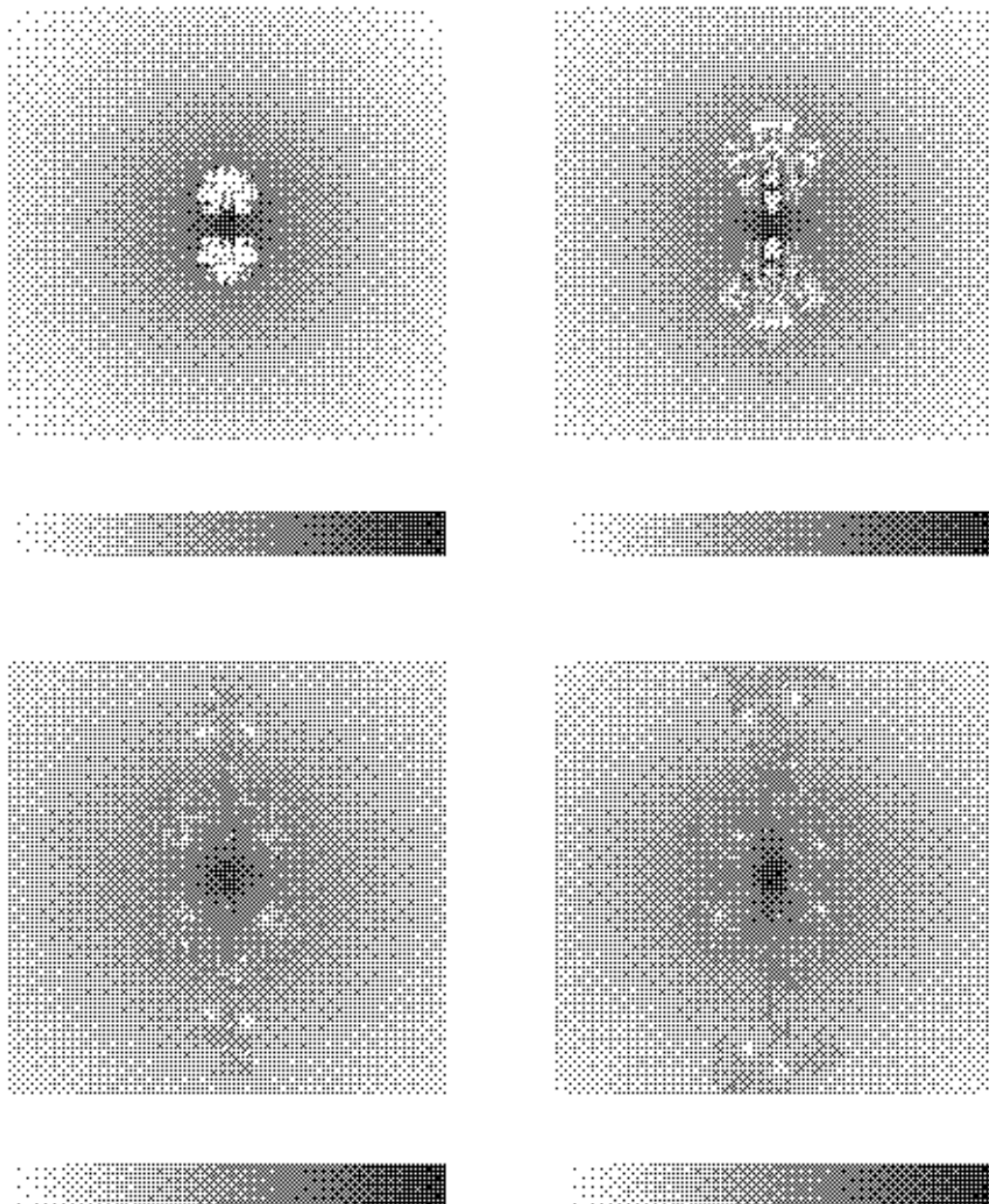


Fig. 3.— Logarithmic contour plots of the density after 84, 167, 252 and 336 Myrs.

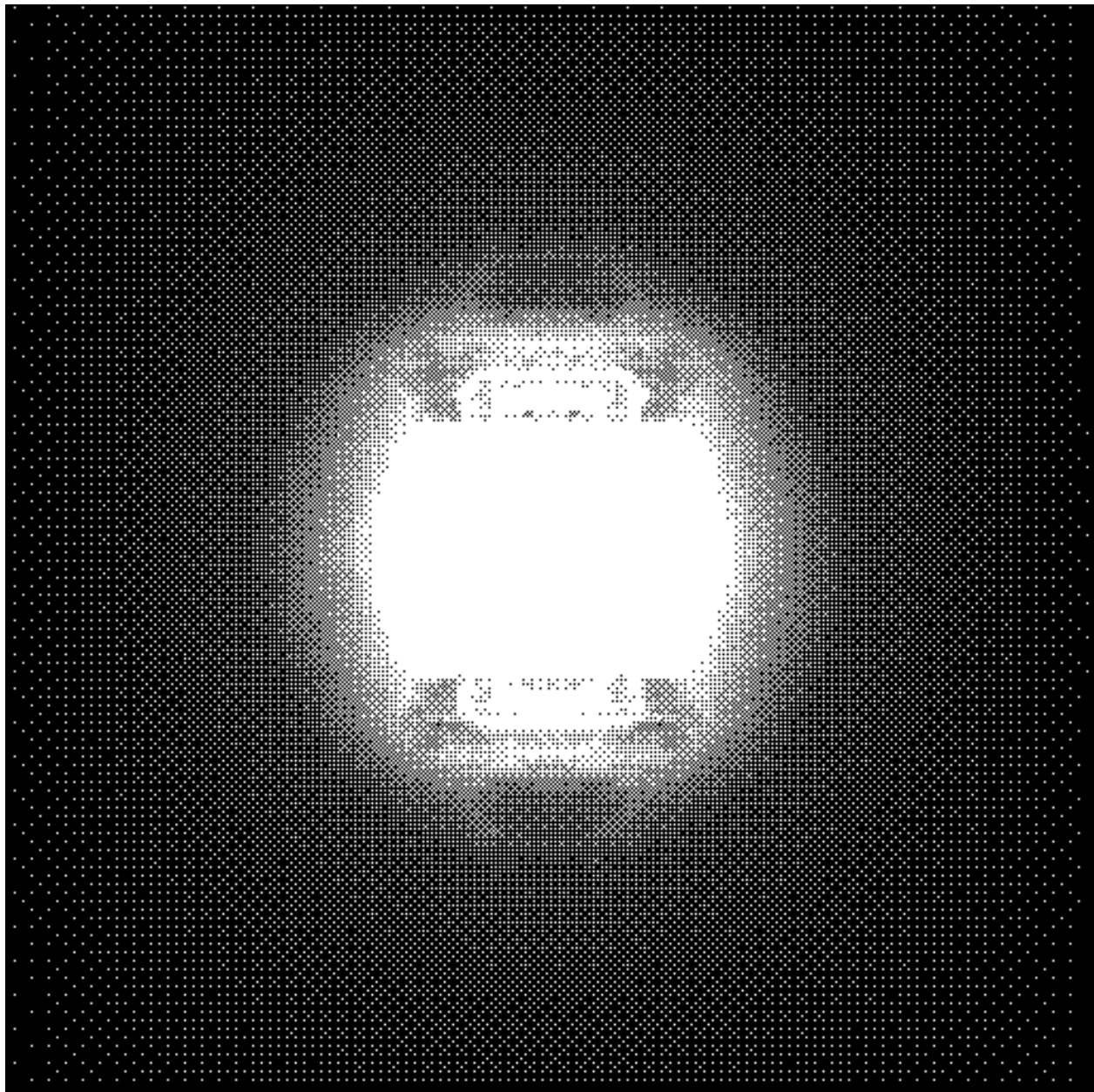


Fig. 4.— Contour plots of the X-ray surface brightness after 100 Myrs. The image covers 140×140 kpc.

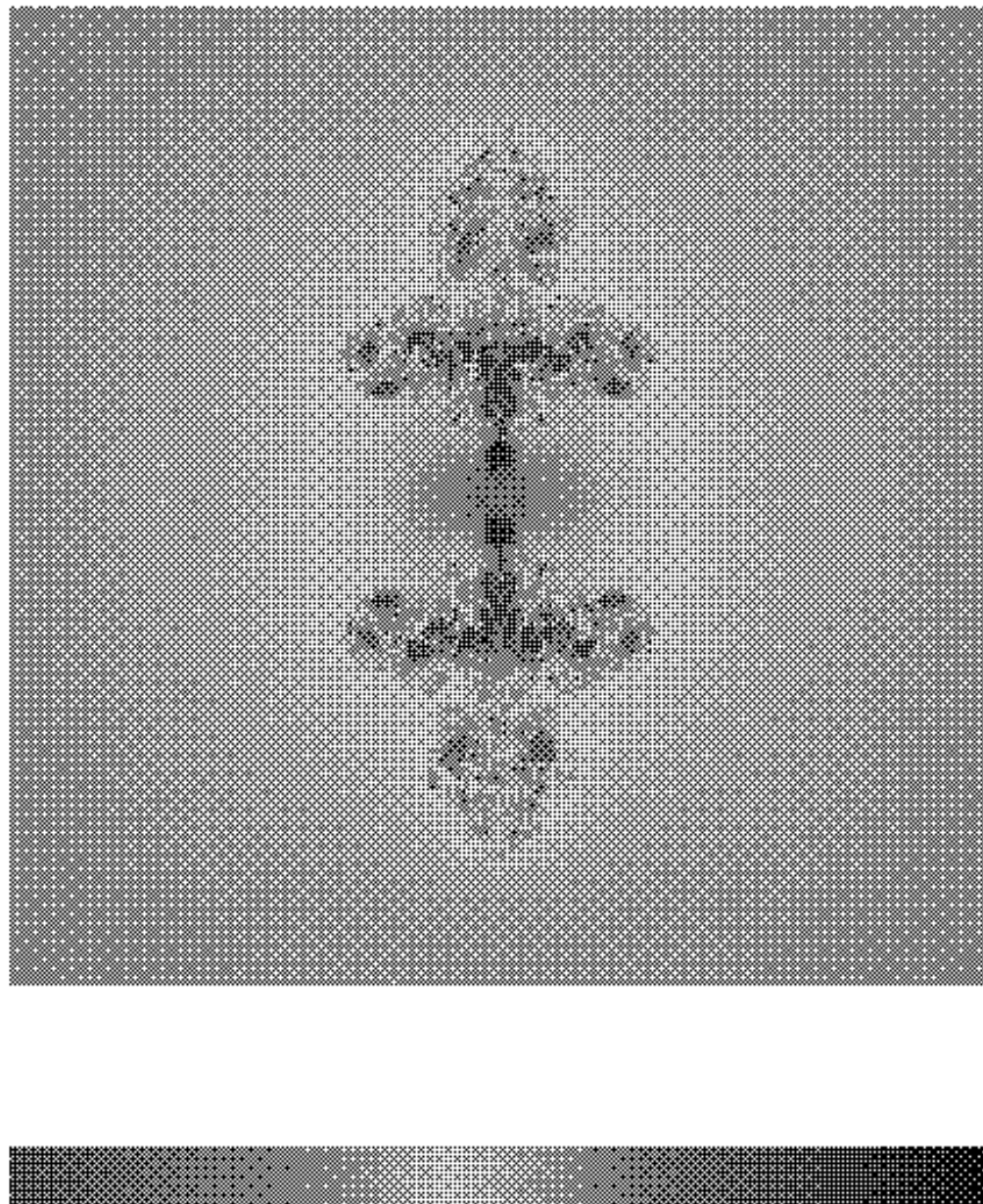


Fig. 5.— Logarithmic contour plots of the temperature after 100 Myrs. The image covers 140×140 kpc.

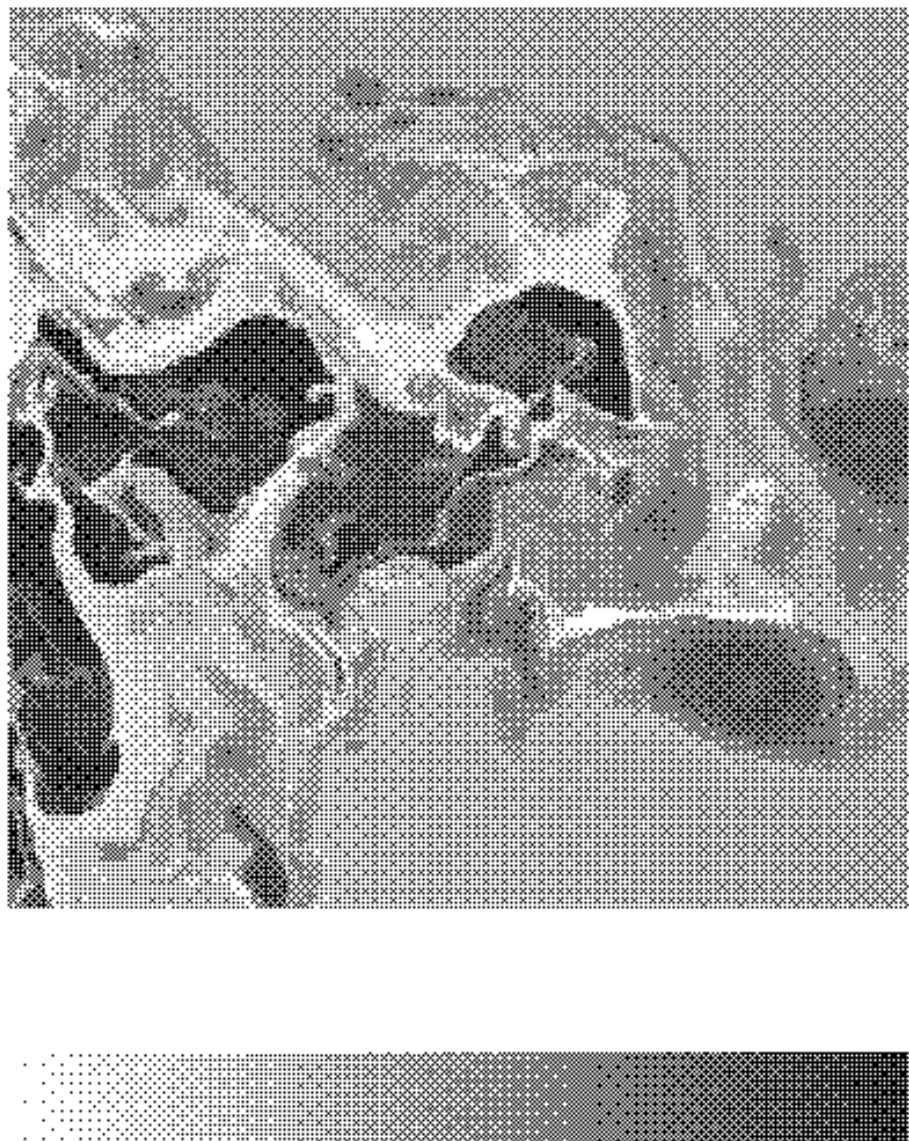


Fig. 6.— Close-up of the temperature around some buoyant bubbles after 100 Myrs. The colder regions around the bubbles correspond to the bright rims seen in X-ray observations.

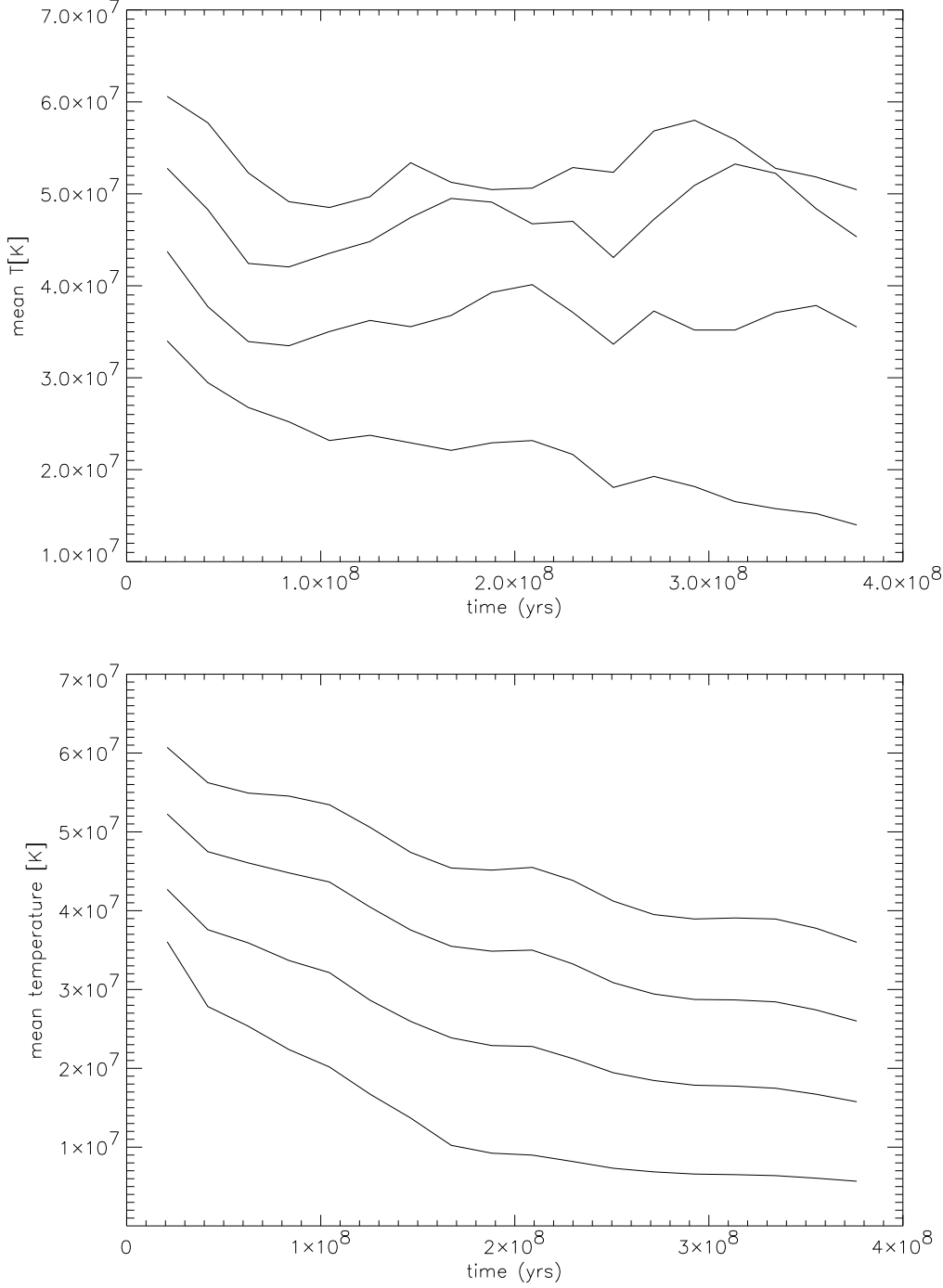


Fig. 7.— Evolution of the temperature that has been averaged over spherical shells about the centre. Each shell has a thickness of 5 kpc. Here the innermost 4 shells are shown which going out to a maximum radius of 20 kpc. The bottom curve corresponds to the innermost shell with the temperature rising as we go farther out. The left panel shows the average temperature in a simulation with heating by bubbles; the right panel shows the average temperature for the identical cluster without heating.

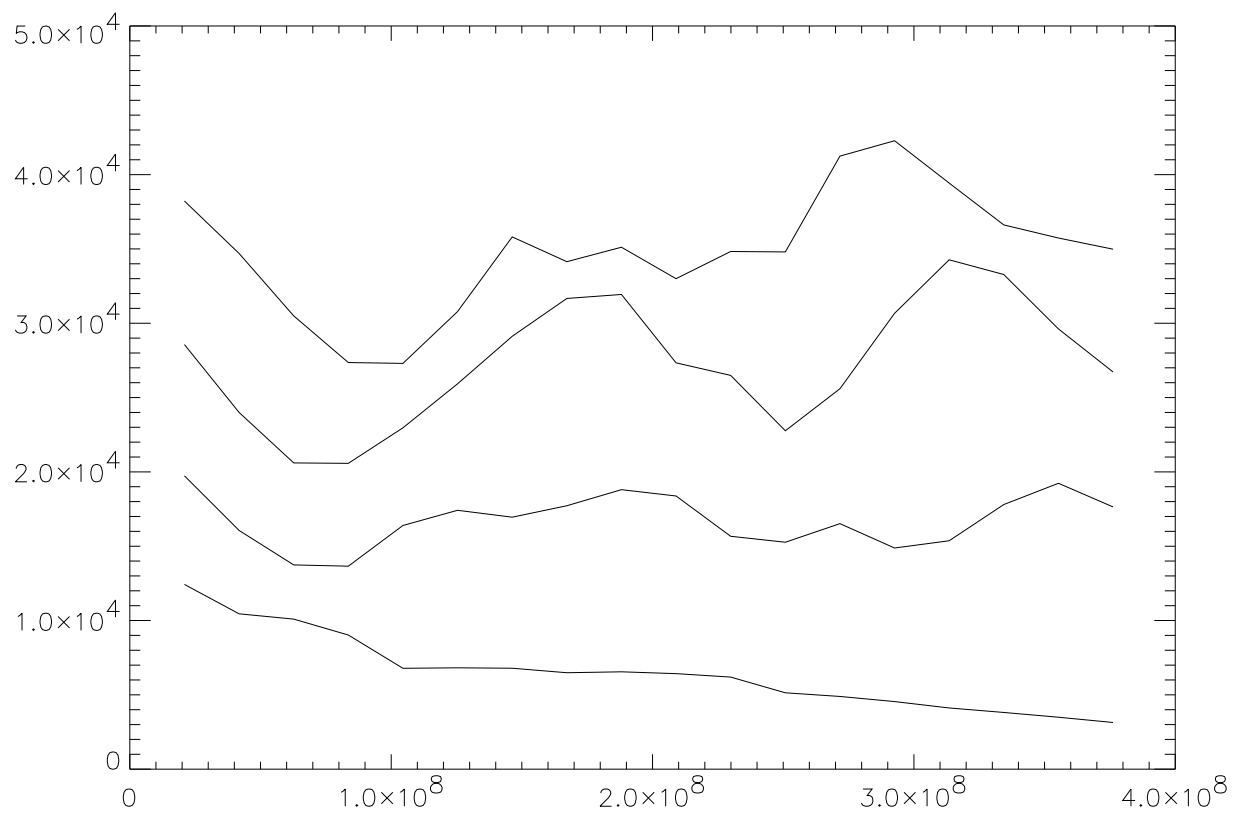


Fig. 8.— Evolution of the specific entropy averaged over spherical shells about the centre. The x-axis shows the time in years.

REFERENCES

Allen, S.W., Taylor, G.B., Nulsen, P.E.J., et al. 2001, MNRAS, 324, 842

Basson, J., & Alexander, P. 2002, submitted to MNRAS

Bertschinger, E., & Meiksin, A. 1986, ApJ, 306, L1

Bicknell, G. V. & Begelman, M. C. 1996, ApJ, 467, 597

Blanton, E.L., Sarazin, C.L., McNamara, B.R., & Wise, M.W. 2001, ApJ, 558, L15

Böhringer, H., Voges, W., Fabian, A. C., Edge, A. C., & Neumann, D. M. 1993, MNRAS, 264, L25

Böhringer, H., Matsushita, K., Churazov, E., Ikebe, Y., & Chen, Y. 2002, A&A, 382, 804

Brighenti, F. & Mathews, W. G. 2002, ApJ, 573, 542

Brüggen, M. & Kaiser, C. R. 2002, Nature, 418, 301

Brüggen, M., Kaiser, C. R., Churazov, E., Ensslin, E. 2002, MNRAS, in press

Burns, J. O. 1990, AJ, 99, 14

Carilli, C. L., Perley, R. A., & Harris, D. E. 1994, MNRAS, 270, 173

Churazov, E., Forman, W., Jones, C., & Böhringer, H. 2000, A&A, 356, 788

, Churazov, E. and Brüggen, M. and Kaiser, C. R. and Böhringer, H. and Forman, W. 2001a, ApJ, 554, 261

Churazov, E., Sunyaev, R., Forman, W., & Böhringer, H. 2002, MNRAS, 332, 729

Churazov, E., Böhringer, H., Brüggen, M., Forman, W., Jones, C., Kaiser, C., & Sunyaev, R. 2002, Lighthouses of the Universe: The Most Luminous Celestial Objects and Their Use for Cosmology Proceedings of the MPA/ESO/, p. 37, 37

Cowie, L. L., Binney, J. 1977, ApJ, 215, 723

Crawford, C. S., Allen, S. W., Ebeling, H., Edge, A. C., & Fabian, A. C. 1999, MNRAS, 306, 857

Fabian, A. C. & Nulsen, P. E. J. 1977, MNRAS, 180, 479

Fabian, A.C. 1994, ARA&A, 32, 277

Fabian A.C., Sanders J.S., Ettori S., Taylor G.B., Allen S.W., Crawford C.S., Iwasawa K., Johnstone R.M., Ogle P.M., 2000, MNRAS, accepted, astro-ph/0007456

Fabian, A.C., Voigt, L.M., & Morris, R.G., 2002, MNRAS, submitted (astro-ph/0206437)

Fryxell, B. et al. 2000, ApJS, 131, 273

Gruzinov, A. 2002, astro-ph/0203031

Mazzotta, P., Kaastra, J. S., Paerels, F. B., Ferrigno, C., Colafrancesco, S., Mewe, R., & Forman, W. R. 2002, ApJ, 567, L37

McNamara, B. R. 1997, ASP Conf. Ser. 115: Galactic Cluster Cooling Flows, 109

McNamara, B. R. et al. 2001, ApJ, 562, L149

McNamara, B. R., 2002, Invited review, "The High-Energy Universe at Sharp Focus: Chandra Science," Symposium at the ASP meeting, 16-18 July, 2001, St. Paul, MN

Narayan, R., & Medvedev, M.V. 2001, ApJ, 562, L129

Navarro, J.F., Frenk, C.S., & White, S.D.M. 1997, ApJ, 490, 493

Nulsen, P. E. J., David, L. P., McNamara, B. R., Jones, C., Forman, W. R., & Wise, M. 2002, ApJ, 568, 163

Owen, F. N., Eilek, J. A., & Kassim, N. E. 2000, ApJ, 543, 611

Peterson, J.R., Paerels, F.B.S., Kaastra, J.S., et al. 2001, A&A, 365, L104

Quilis, V., Bower, R. G., & Balogh, M. L. 2001, MNRAS, 328, 1091

Raymond, J. C., Cox, D. P., & Smith, B. W. 1976, ApJ, 204, 290

Reynolds, C. S., Heinz, S., & Begelman, M. C. 2001, ApJ, 549, L179

Ruszkowski, M., & Begelman, M. 2002

Sarazin, C. L. 1986, Reviews of Modern Physics, 58, 1

Sarazin, C. L. 1988, NATO ASIC Proc. 229: Cooling Flows in Clusters and Galaxies, Kluwer, Dordrecht, 1

Saxton, C. J., Sutherland, R. S., & Bicknell, G. V. 2001, ApJ, 563, 103

Schindler, S., Castillo-Morales, A., De Filippis, E., Schwope, A., & Wambsganss, J. 2001, A&A, 376, L27

Soker, N. & Sarazin, C. L. 1990, ApJ, 348, 73

Tabor, G., & Binney, J. 1993, MNRAS, 263, 323

Tamura, T., Kaastra, J.S., Peterson, J.R., Paerels, F., et al. 2001, A&A, 365, L87

Voigt, L.M., Schmidt, R.W., Fabian, A.C., Allen, S.W., & Johnstone R.M., 2002, MNRAS, submitted (astro-ph/0203312)

Voit, G. M. & Bryan, G. L. 2001, Nature, 414, 425

Vrtilek, J. M., David, L. P., Grego, L., Jerius, D., Jones, C., Forman, W., Donnelly, R. H., & Ponman, T. J. 2000, Constructing the Universe with Clusters of Galaxies,

Wilson, A. S., Young, A. J., & Shopbell, P. L. 2000, ApJ, 544, L27

Zakamska, N.L. & Narayan, R., 2002, ApJ, in press